LRP 791/04 November 2004

Front steering ECCD launcher study for the ITER upper port

M.A. Henderson, R. Chavan & F. Sanchez

ISSN 0458-5895

Front Steering ECCD Launcher Study for the ITER Upper Port

10 June 2004
(final version 16 November 2004)

M.A Henderson, R. Chavan, F. Sanchez
CRPP - EPFL

The use of front steering (FS) launcher in the upper port of ITER was studied with the goal of decreasing the projected beam's spot size at the resonance for improved efficiency in NTM stabilization on both the q=2 and 3/2 rational magnetic flux surfaces. The present design (non optimized) offers a factor of 1.4 improvement in efficiency ($\propto j_{CD}$) using a modulated co-ECCD beam and a factor of $\geq$2.0 in efficiency ($\propto j_{CD}/w_{CD}$) for non-modulated co-ECCD beam relative to the current remote steering (RS) launcher. Also, the steering capabilities has increased by a factor of 1.4, achieving localized co-ECCD deposition on the q=2 and 3/2 for the Gribov, sob2 (l_i=1 & 0.7), sob3 (l_i=0.7) and sob5 (l_i=0.7) equilibriums.

FS Launcher Study

1) Introduction

This report concludes the study performed by CRPP that considers the implementation of a front steering (FS) launcher in the ITER upper port. The goal of the study was to consider if a FS launcher could improve the characteristics of the ECRH beam for NTM stabilization. In particular, an attempt was made to improve the following parameters relative to the present remote steering (RS) launcher design[1], with the main imporvement consisting of:

1) Reduce the spot size at both the q=2 & 3/2 resonance location

2) Increase scanning angle

3) Consider other possible ECH or ECCD scenarios

This document is not a stand alone item but relies on the previous FS reports (attached as appendices), which offer details concerning: the design strategy (Appendix A), general design (Appendix B), optimization procedure (Appendix C) and power densities on the mirrors (Appendix D).

The greatest challenge of the FS launcher is the realization of a reliable steering mechanism. However, before investing the time and effort in designing a reliable steering mechanism, it is prudent to investigate if there can be a significant improvement in the steering range and reduction of the spot size at the resonance. This report, therefore, concentrates on only the beam optics of the FS launcher. If the FS launcher offers significant improvement over the RS launcher, then an engineering study of the steering mechanism would be merited. This present study utilizes a modified steering mechanism (see Appendix B) based on the one proposed previously by R. Chavan[2].

The design work has not yet been incorporated in a CATIA format. All figures and calculations have used port dimensions coming from CATIA[3] and transfered to a MATLAB program. As a result all figures in this report will be presented in 2D.

The FS launcher in its present state is not optimized. There is more space around the mirrors than initially envisioned, which can be used to increase the mirror sizes and obtain an even small beam size at the resonance layer. Instead of further optimizing, the design was frozen at its present state in order to compile this report.

The outline of this report is as follows: a general description of the present launcher design is provided in Section 2. The realized beam optics are compared with the RS launcher in section 3. In section 4, the NTM stabilization efficiency is defined and estimated for the FS and RS launchers. A brief discussion on neutron shielding is presented in section 5 followed by other possible FS launcher scenarios in Section 6. A conclusion is given in section 7.

2) The current FS launcher design

---

1. *Revision of design incorporating physics based performance analysis*, B.S.Q. Elzendoorn *et al*, Deliverable 2003-2004 (a).3, April 2004.
2. R. Chavan, "Support of the Design of the ITER ECH&CD System: Design of the Upper Port Launcher", EFDA/02-687 CRPP-EPFL.
3. FZK model: v1_19_05_04.zip

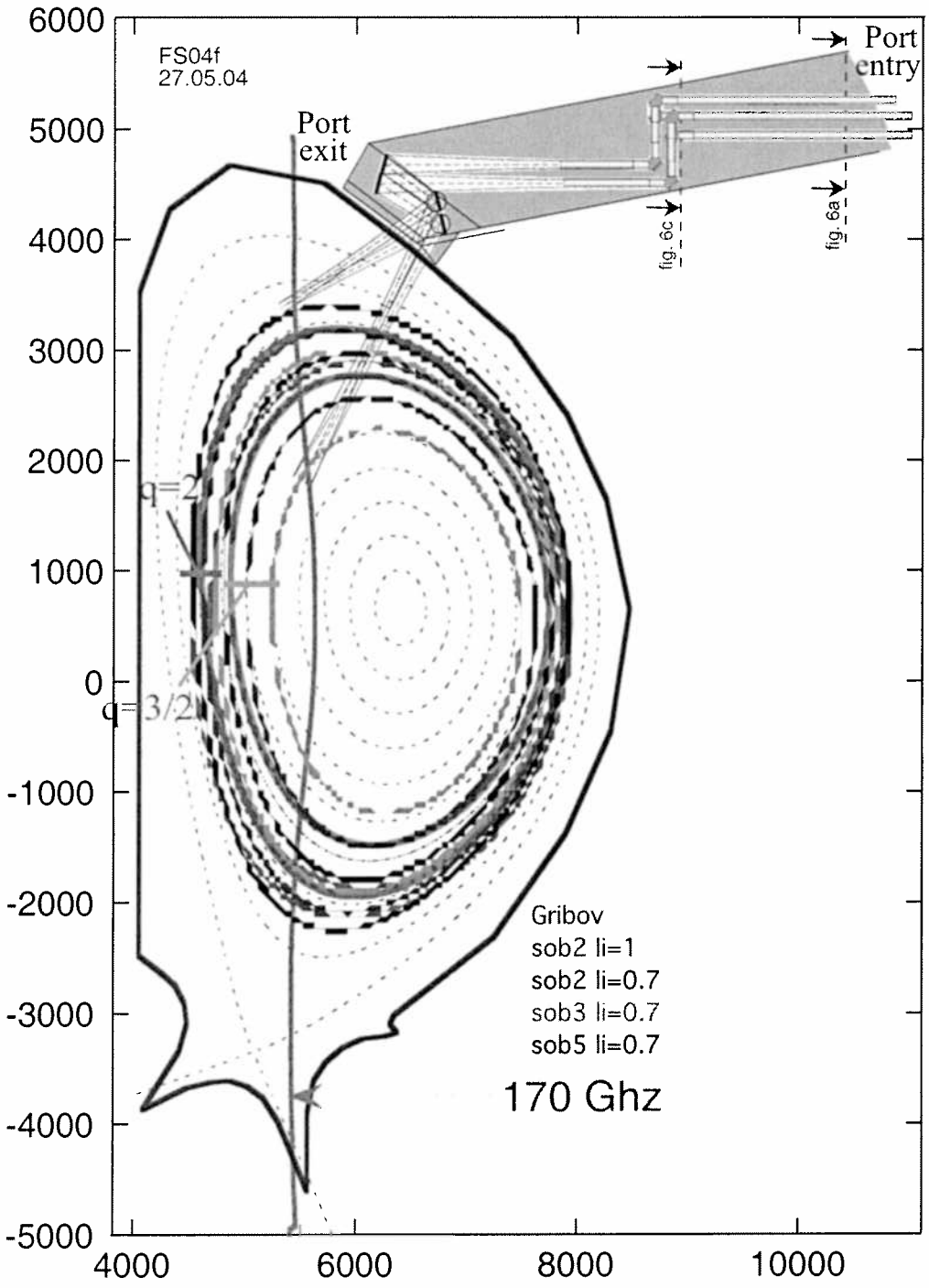

Figure 1 Poloidal cross section of the ITER plasma along with the FS launcher installed in the upper port. The launcher is designed to steer the RF beam from Z~1.8m to 3.4m along the nearly vertical resonance surface. This scanning region includes all of the q=2 and 3/2 flux surfaces for the 5 ITER equilibriums shown. Note the port entry refers to the right side and the port exit is on the left (plasma) side.

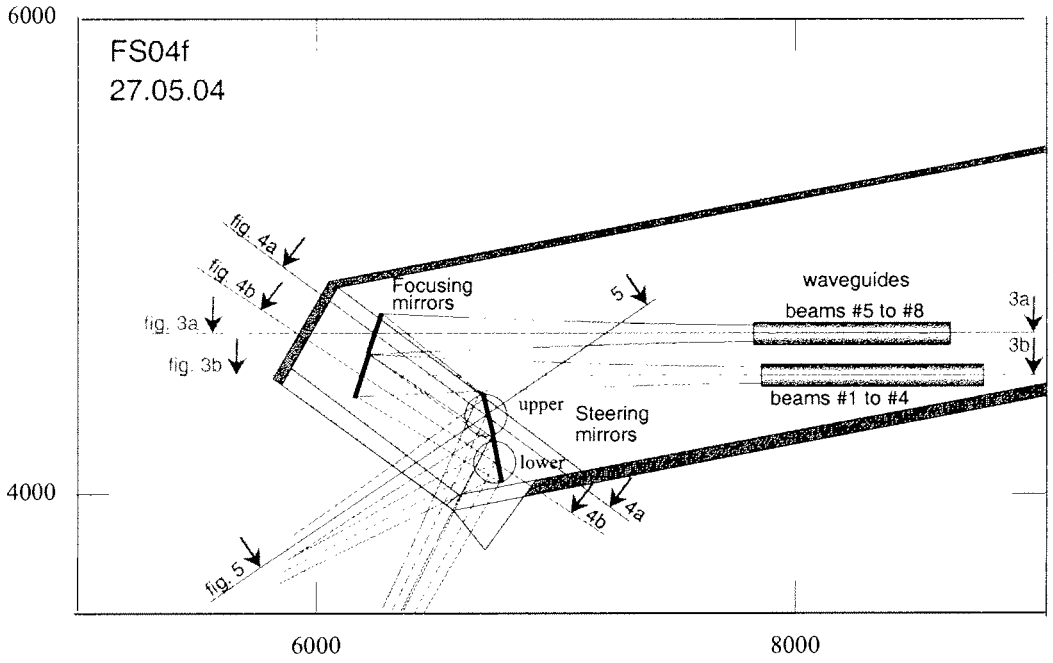

Figure 2 The FS launcher uses a two mirror system to focus (1st mirror) and steer (2nd mirror) an RF beam toward the plasma. Three different cuts are provided: figures 3 (waveguide to steering mirror plane), figure 4 (plane defined by the two mirrors) and figure 5 (plane of the injected beam into the plasma). An additional vertical view of the waveguide arrangement at the port entrance and before the miter bends (see previous figure) is given in figure 6.

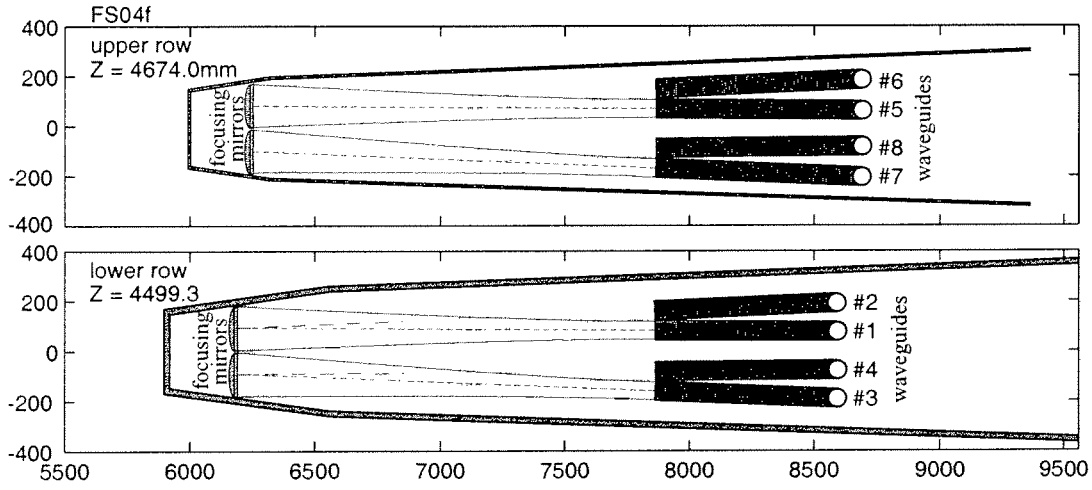

Figure 3 Horizontal view of the waveguide - focusing mirror plane defined in figure 2. Each two waveguide set directs the beams toward the center of each focusing mirror. The output beams are titled by ~±1.4° and results in a toroidal spread of the injected beam by $\Delta\beta<1.5°$. The toroidal spread can be reduced by varying the waveguide tilt, the incident offset position on the focusing and steering mirrors, and the relative poloidal injection angle between the two mirrors

A view of the FS launcher in the poloidal plane along with the plasma cross section and the q=2 and 3/2 surfaces for a variety of plasma equilibriums is shown in figure 1. There are four upper (blue) and four lower (red) beams superimposed in figure 1. A two mirror assembly is used to focus (first mirror) and steer (second mirror) the beam for localized deposition at the desired flux surface along the nearly vertical resonance layer. An expanded view of the two mirror system is shown in figure 2. The horizontal cut along the waveguide axis (identified by the blue and red dashed lines of figure 2) is shown in figure 3(a) and (b), where the beam from the two waveguides are aimed at the center of a focusing mirror. The reflected beams are then directed downward to the steering mirror. The titled plane between the two mirrors is shown in figure 4(a) and (b) as viewed from the plasma. There are four beams incident on each steering mirror, which is divided into two sections, see figure 5. Each section is tilted to inject the two beam with a $\beta=20^{\circ}$ into the plasma. The two beams incident on each half section are offset from the center by ±15cm. The two half sections form nearly parallel planes, a slight ridge is formed between the two sections, see figure 5.

2.1) waveguide

The present FS launcher design is compatible with either 63.5mm or 45mm (inner diameter) waveguide. The larger waveguide diameter was chosen as the base design, since it does not require the use of a down taper[1] (transmission line will use the 63.5mm waveguide), and in addition it offers a lower power density on the miter bend mirrors. Note for the 45mm waveguide, existing ECH transmission lines operate reliably with 1.0MW in 31.75mm waveguide, equivalent to 2.0MW in 45mm waveguide.

The base design also includes a pair of miter bends, which decreases the down streaming of neutrons in the waveguide. The miter bend assembly adds an additional ~1.0% transmission loss, which doubles the losses associated with the FS launcher (neglecting the mode conversion losses at the waveguide opening).

The waveguide at the port entry is arranged in three rows with two waveguides in the upper row and three in the middle and bottom rows as shown in figure 6a (The approximate location of the viewing planes of figure 6 are shown on figure 1). This arrangement allows ample space for insertion of an in-line gate valve avoiding conflict between the gate valve actuators and neighboring waveguide lines (see figure 6b). The waveguides remain horizontal up to the miter bends in the launcher, however, the waveguides are angled in the horizontal plane, to compress the inter-spacing between the waveguides as they approach the narrow upper region of the port (see figure 6b).

The waveguide sections between the miter bends are vertical and approximately 600mm in length. The last section of the waveguides are in a horizontal plane and angled by $\pm 1.4^{\circ}$ with the emitted beam from the waveguide aiming at the center of the focusing mirror. The tilt creates the ±15mm offset of the two beams on the steering mirror (discussed above, see figure 4), which maintains a low the peak power density, while decreasing the overall size of the mirror surface (see Appendix C). The beams also have a spread in the injected toroidal angle ($\Delta\beta \sim \pm 1.5^{\circ}$). Due to the Doppler shift of the resonance, the two beams are no longer

1. The down taper could result in a reflection of some of the higher order modes in the transmission line. Breakdown in the waveguide may occur, if the superposition of the reflected and forward propagating modes occur on the diamond window or miter bend surfaces. Also, the forward propagating higher order modes in the line may be absorbed in the down taper resulting in potentially over heating the down taper.

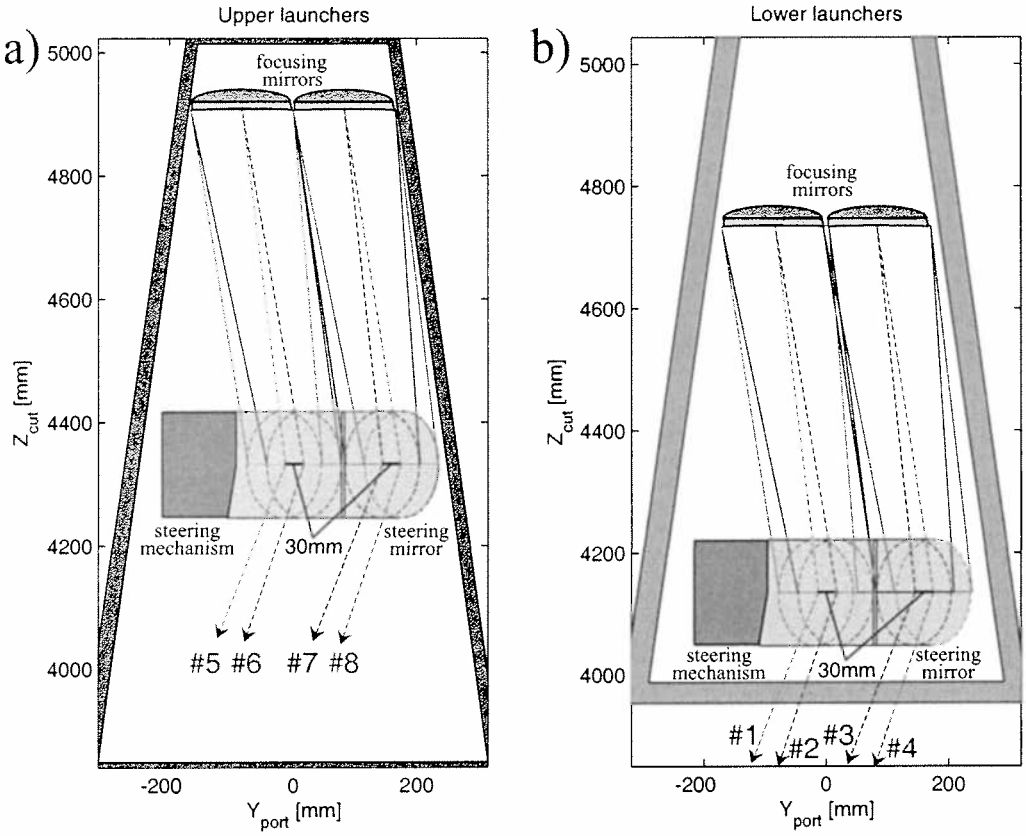

Figure 4 Plane view of the RF beams between the focusing and steering mirrors. Two beams are incident on the center of the focusing mirror, and then directed downward to the steering mirror. The steering mirror is divided into two sections, with two beams incident on each half section and offset by 15mm.The RF beams are then directed toward the plasma with a toroidal injection angle of $\beta=20\pm1.5°$.

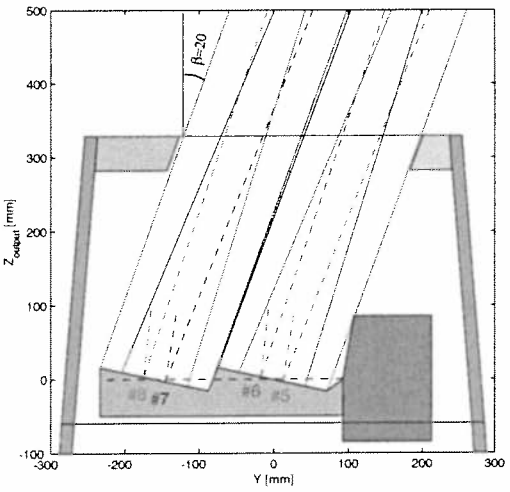

Figure 5 Cross sectional view of the steering mirror. A ridge separates the two nearly parallel half sections of the steering mirror (in this case Upper launcher). The lower launcher is similar but with more free space between the port wall and steering mirror assembly. The toroidal extent of the opening in the front panel is ~330mm in width. Note: there is a large margin of space around the mirror which could be used to increase the mirror size and beam spot size on the mirror and further reducing the beam size at the resonance surface.

deposited on the same flux surface, resulting in a broadening of the deposition width, as shown in figure 7a and b. This can be avoided by adjusting the vertical position of the two waveguides, so that the incident beams on the focusing mirrors will be reflected at different poloidal angles resulting in equivalent deposition location. Optimizing the poloidal angle offset will require multiple runs of either a ray tracing or beam tracing code, which is outside the scope of this initial study. As a rough estimate, using the q=2 and 3/2 launching geometry where the deposition changed by $\Delta\rho\sim0.1$ for a change in the poloidal injection angle of $\Delta\alpha \sim10^{\circ}$, implies a poloidal correction of $\alpha_{opt}\pm0.12^{\circ}$ for superimposed radial deposition of the two beams. The spread in β will also be reduced by decreasing the offset distance on the steering mirror. As shown in figure 6, there are a few centimeters of space between the steering mirror and the inside port wall. The beam size on the steering mirror can be increased, which lowers the power density on the mirror and can reduce the beam spot size at the plasma resonance layer. The two beams can then be brought closer together, decreasing both the offset spacing and the toroidal angle spread. Also, the design maintained a peak power density of $320W/cm^2$ (See Appendix D). The offset distance and beam spread would be reduce if this constraint is relaxed. (Note: the maximum power density on the steering mirror is ~1/5th that of the maximum power density on the plasma facing mirror of the RS launcher).

2.2) Focusing mirror

The characteristics of the focusing mirrors are given in table 1, where ω_{ow} and ω_{op} refer to the beam waist at the end of the waveguide and in the plasma, d_{wf} and d_{f0} are the corresponding distance from the waveguide to the focusing mirror and focusing mirror to the beam waist in the plasma, ω_f is the spot size on the mirror and θ_i is the incident beam angle on the mirror. The curvature of the mirror is defined as an ellipsoid of revolution characterized by the major and minor radius (A and B) also given in Table 1. The mirror diameter[1] is taken as $3.5*\omega_f$. The mirror is to be made of copper and is entirely hidden from the plasma with a minimum shielding thickness of ~15cm. The peak power density assumes the absorbed power fraction as outlined in Appendix D: *Power Density on plasma facing mirror*[2].

The design of the cooling circuit is not included in the scope of this study, a similar cooling system as used for the plasma facing mirror of the RS launcher can be used for the focusing mirror. The peak power density is estimated from the minimum beam spot size on the mirrors and is proportional to $2*(\omega_{f\text{-}RS}/\omega_{f\text{-}FS})^2$, where the factor of "2" compensates for two beams incident on the FS focusing mirror. The peak power density of one beam on the RS mirror is a factor of ~4.9 higher than for the two superimposed beams on the FS focusing mirror.

The focusing mirror is fixed in place rigidly to the launcher assembly. The method of attaching the mirror to the launcher assembly structure is not included in the scope of this study.

---

1. The FS design used $3.5*\omega_f$ for direct comparison with the RS launcher design (26th Nov. 2003 design report). The current RS launcher design (April 2004) now uses $3.0*\omega_f$.
2. The original document is included in Appendix D, which used an absorption power coefficient of 0.0035.

Table 1: Parameters of the focusing mirrors

Parameter	Upper Launcher	Lower Launcher
(R,Z) position [mm]	(6242.8, 4674.0)	(6191.6, 4499.3)
ΔY, offset from port axis [mm]	83.0	83.0
d_{wf}, input [mm]	1588.4	1670.6
w_{ow}, input [mm]	20.431	20.431
d_{fo}, output [mm]	1319.0	1707.0
w_{op}, output [mm]	21.000	21.000
θ_i [°]	18.25	16.75
w_f [mm]	48.19	50.24
A [mm]	1969.7	2035.3
B [mm]	1870.4	1948.7
R_{in} [mm]	1913.3	2001.6
R_{out} [mm]	1979.3	2069.0

Where d_{wf} is the distance from the waveguide to the focusing mirror center, w_{0w} is the beam waist at the waveguide aperature, d_{f0} is the distance from the mirror to the beam waist (w_{op}), θ_i is the beam's incident angle on the mirror, w_f is the beam spot size on the mirror, A and B are the major and minr axis of the elipse, R_{in} and R_{out} are the input and output radius of curvitures of the beam.

2.2) Steering mirror

An outline drawing of the upper launcher steering mirror is shown in figure 5, viewing from the cut illustrated in figure 2. The lower launcher (not shown) is equivalent but with additional space between the port wall and steering mirror assembly. There are four beams incident on the mirror, which is divided into two surfaces. Each surface is inclined so that the average toroidal injection angle is 20°. The two beams incident on each inclined surface are offset ±15mm from the center. The partial overlap of the two beams reduces the size of the mirror (in the toroidal direction), while only increasing the peak power density by >10%. The aixs of rotation of the steering mirror intersects the center of each half mirror surface.

The steering mechanism is the critical component of the front steering launcher. This study investigates only the improved beam optic parameters of the FS launcher relative to the RS launcher. The engineering aspects of the design are left for a future study. Herein, a modified steering mechanism is used as proposed by R. Chavan[1]. The diameter of the steering

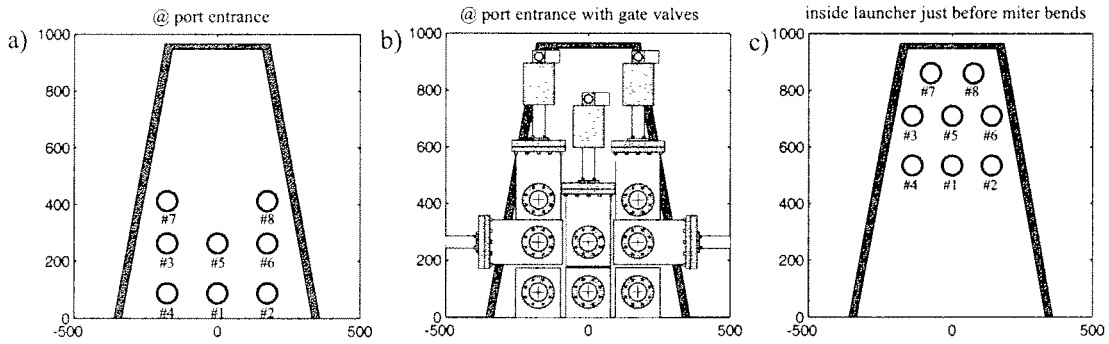

Figure 6 (a) The waveguide arrangement at the entrance into the upper port. (b) The enter waveguide spacing is sufficient to allow the introduction of in-line gate valves, note there is no conflict between the waveguide and gate valve actuators, note that the actuators in the bottom row point downward and are not shown. (c) The axis of the three rows of waveguides are in a horizontal plane. The waveguides are slightly titled to compress the horizontal distance between axis as the waveguides approach the miter bend (the port is narrower on top),

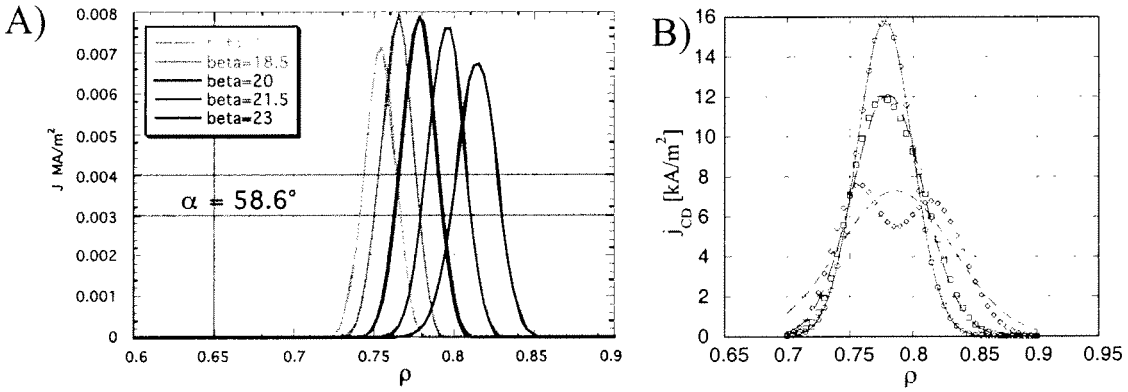

Figure 7 (a) Due to the Doppler shifted resonance, beams with different toroidal injection angles, β, (and similar poloidal angles) will be deposited at different radial locations. The two beam set have a toroidal angle spread of $\Delta\beta \sim 1.5°$, which will result in a widening of the effective deposition width. This can be reduced by optimizing the poloidal injection angle of each beam and/or decrease the offset distance of the beams on the steering mirror.1.0MW per beam was used in the ECCD calculations.

mechanism would be increased (from 140 to 170mm) and the length decreased (from 196 to 120mm), maintaining the same potential poloidal steering range (±20°).

The mirror is made of copper (equivalent with the RS design). However, since the mirror is plasma facing, alternative material such as Tungsten or a Molybdenum alloy should be considered, which offers a lower sputtering yield. (note: the choice of an optimum plasma facing material is not included in the scope of this study.) The steering mirror is recessed back into the port by ~30cm, which reduces the sputtering of particles into the plasma.

The beam and steering mirror parameters are give in table 2. The peak power density of the two overlapping beams are a factor of ~4.5 lower tan on the peak power density of the plasma facing mirrors of the RS launcher

Table 2: Parameters of the steering mirror

Parameter	Upper Launcher	Lower Launcher
(R,Z) position [mm]	(6705, 4332)	(6742, 4135)
d_{fs} [mm]	575.0	660.0
α_o [°]	49.4	44.7
$\Delta\alpha$ [°]	±15.0	17.1
β_o [°]	20.0	20.0
$\Delta\beta$ [°]	1.46	1.41
ω_s [mm]	35	35
ω_o [mm]	21.0	21.0
d_{so} [mm]	1047.5	1047.5

Where d_{fs} is the distance from the focusing to the steering mirror center, α_o and $\Delta\alpha$ is the center and steering range of the poloidal angle, β_o is the average toroidal injection angle, Δb is the range in the offset toridal angle, ws is the spot size on the mirror, w_o is the beam waist in the direction of the plasma and dso is the distance from the steetring mirror to the beam waist.

3) Beam characterization

The main goal of this study was to investigate if a front steering launcher could provide a wider scanning range and a narrower deposition width relative to a remote steering launcher. If a significant improvement in the beam parameters is obtained, than there would be more motivation to solve the engineering complexities of the steering mechanism in the harsh environment in the ITER upper port.

In general, the deposition width at the resonance can be reduced by projecting the beam waist far into the plasma. The larger the beam spot size on the focusing mirror, the farther the beam waist can be projected into the plasma. A large beam spot size on the mirror is

1. *Support of the design of the ITER ECH&CD System: Design of the Upper Port Launcher*, R.Chavan.

obtained by increasing the distance between the waveguide aperture and the focusing mirror. This distance is limited for the RS launcher due to the steering range of the exiting beam from the waveguide.The mirror would has to be considerably larger to "catch" the beam at all angles it is emitted from the RS waveguide. However, for the FS launcher, the beam can expand to a factor 2 or 3 larger than for the RS launcher, while maintaining a moderately sized focusing mirror[1]. The beam waist can then be projected ~1.5m in the direction of the plasma. The size of the focusing mirror is limited by the narrow region within the port.

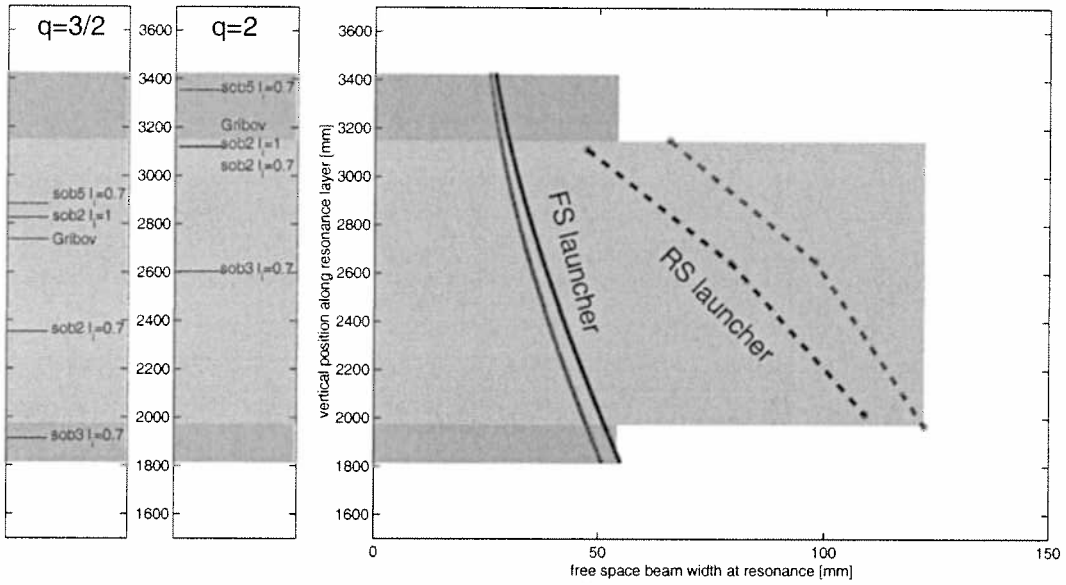

Figure 8 The calculated beam radius (e^{-1} in E-field) in free space along the vertical resonance for both the FS launcher (solid lines) and the RS launcher (dashed lines), where blue (red) corresponds to the upper (lower) launchers. The large blue (red) band corresponds to the vertical region accessible by the steering range of the FS (RS) launcher. The vertical location along the resonance surface of the q=3/2 and q=2 is shown on the left for the different ITER equilibrium. The FS launcher delivers a narrower beam over a larger region compared to the RS launcher.

For a given spot size on either the focusing or steering mirror, the size and location of the beam waist can be optimized to minimize the deposition width at the resonance[2]. The resulting free space beam radius (e^{-1} in E-field) is shown in figure 8 as a function of the estimated vertical deposition location (the intersection of the 170GHz resonance surface and the center line of the beam propagated in free space). The upper and lower launchers are indicated by the blue and red (solid) lines along with the equivalent for the RS launcher[3] (dashed lines). The vertical intercept between the q=2 and 3/2 flux surface and the resonance surface is indicated on the left for the five equilibriums of concern for the NTM stabilization. Typically, the average FS launcher beam waist is at a maximum half the size of the average RS beam waist, and in addition the FS launcher spans a larger region (a factor of 1.4 increase over the RS launcher) and encompasses all desired q=2 and 3/2 for the Gribov, sob2 (l_i=1 & 0.7), sob3 (l_i=0.7) and sob5 (l_i=0.7) equilibriums.

1. The FS focusing mirror is ellipsoidal in shape with axis of ≤176mm and 184mm. The RS plasma facing mirror is ≤630mm and 80mm.
2. Optimization process outlined in Appendix C: *FS launcher Status Report #2* (02.04.04).
3. RS launcher beam radius calculated based on beam characteristic described in *Revision of design incorporating physics based performance analysis*, B.S.Q. Elzendoorn *et al*, Deliverable 2003-2004 (a).3, April 2004.

The steering range was chosen to provide q=2 and 3/2 co-ECCD for the desired plasma equilibrium above. The scanning range can easily be increased toward larger Z(res) (or ρ) values without increasing the size of the beam waist. However, the lower Z(res) values are near the limit, access to inner flux surfaces increases the incidence angle on the steering mirror, requiring a larger mirror size in the vertical direction. The current design maintains a 20mm spacing between the steering mirror and floor of the port wall, which would be compromised if the vertical size of the mirror was increased. Also, the beam radius at the resonance can be further optimized depending on the available space between the mirror structure and the inside port wall (see figures 4 and 6) and the maximum allowable power density of the focusing and steering mirrors. Further optimization can be performed once the current FS design is incorporated in the CATIA drawings.

4) NTM stabilization figure of merit

The principle role of the upper port ECRH launcher is to stabilize the NTMs by delivering current inside either the q=2 or q=3/2 magnetic island using co-ECCD. The effectiveness of the beam to stabilize the NTM depends on the ECCD deposition width (w_{CD}) relative to the marginal island width (w_{marg}), and the co-ECCD current density (j_{CD}) relative to the bootstrap current density (j_{BS}) just outside of the island. A figure of merit for the NTM stabilization efficiency can then be described as:

$$\eta_{CD} \propto \frac{j_{CD}}{j_{BS}} \frac{w_{marg}}{d_{CD}}$$

Since j_{BS} and w_{marg} are independent of the launcher choice, the figure of merit for a given ECCD launching system can be described as

$$\eta_{CD} \propto \frac{j_{CD}}{d_{CD}}$$

This relation is applicable when the co-ECCD is not modulated. In the modulated case, the co-ECCD is turned on only when the island is located at the deposition location. In this case only the local current density inside the island is important:

$$\eta_{CD} \propto j_{CD}$$

The relation between the free space beam radius and the calculated j_{CD} and w_{CD} dimension has been estimated by varying the location of the beam waist relative to the resonance location while keeping all other beam and launching parameters constant (see figure 9a)[1]. The launching configuration corresponded to a nearly equivalent FS launcher design for q=3/2 co-ECCD deposition. The relation between the local free space beam radius and the calculated peak current density and deposition width is shown in figure 9b. Although the relation corresponds to the specific launching geometry for the q=3/2 Gribov equilibrium, the equivalent relation for q=2 heating was nearly identical. An additional scenario was simulated with an infinitely thin beam, where $\omega_E = 0$, along the entire beam trajectory. The peak current density and deposition width approaches some finite value due to geometrical effects. The Doppler shifted resonance spreads the absorption over multiple flux surface due to the non-

1. Ray tracing calculations provided by D.Farina et al, S.Nowak, G.Ramponi *et al*, *Local beam size effect on the width of the driven current density profile*, 8 April, 2004.

tangential angle of the beam relative to the flux surface at the Doppler shifted resonance location. As ω_E approaches large values, the peak current density and absorption width are limited by the physical size of the beam.

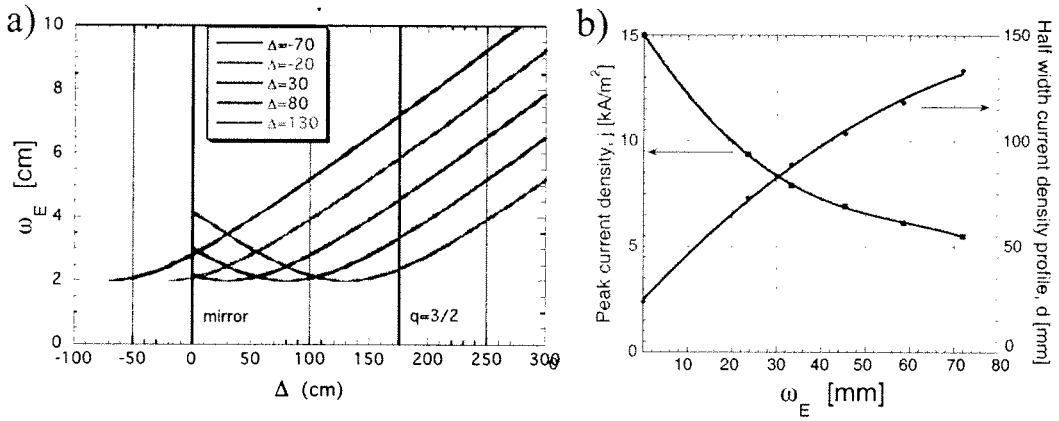

Figure 9 (a) The beam waist location relative to the q=3/2 resonance layer was scanned so as to vary the free space beam width at the q=3/2 resonance layer with 1.0MW of injected power. (b) Then the relative dependence of the calculated peak driven current density and deposition width on the free space beam width at the resonance layer can be approximated.

The relation between j_{CD} and w_{CD} of figure 9(b) can be correlated to the local free space beam radius of figure 8, yielding a direct comparison of NTM stabilization efficiency of the RS and FS launchers, see figure 10a and b. Note the near tangential injection to the resonance surface would increase the effective beam width. However this was not tken into account. Also the beam divergence will be slightly larger, which may increase the spreading of the beam. Therefore, the estimate probably over estimates the peak current density and underestimates the deposition width for the RS launcher. The FS launcher provides greater than a factor of 2 (1.4) in improved NTM stabilization efficiency over the entire range of the non-modulated (modulated) co-ECCD deposition relative to the RS launcher (averaged between upper and lower launchers).

These estimates assume that the same power is used for both RS and FS launchers, however, the power densities on the FS launcher mirrors are at least a factor of 4 lower than the RS launcher mirrors. If at high power densities, the RS launcher mirror is limited to transmitted power below 2.0MW, than the effective NTM stabilization efficiency will decrease due to the lower allowable injected power. A comparitive NTM stabilization efficiency of the two launchers will be then proportional to $j_{CD\text{-}FS} * P_{FS} / j_{CD\text{-}RS} * P_{RS}$, where P_{FS} and P_{RS} are the maximum allowable injected power into the launcher.

5) Neutron shielding

The following aspects were taken under consideration in designing the FS launcher:

1) Minimize the opening in the front shield
2) Keep the waveguide "line-of-sight" as far off-axis as possible
3) Maximize the neutron shielding of the waveguide aperture and focusing mirror.
4) Recess the steering mirror and mechanism as far from the plasma as possible.
5) Minimize the empty space within the port plug.

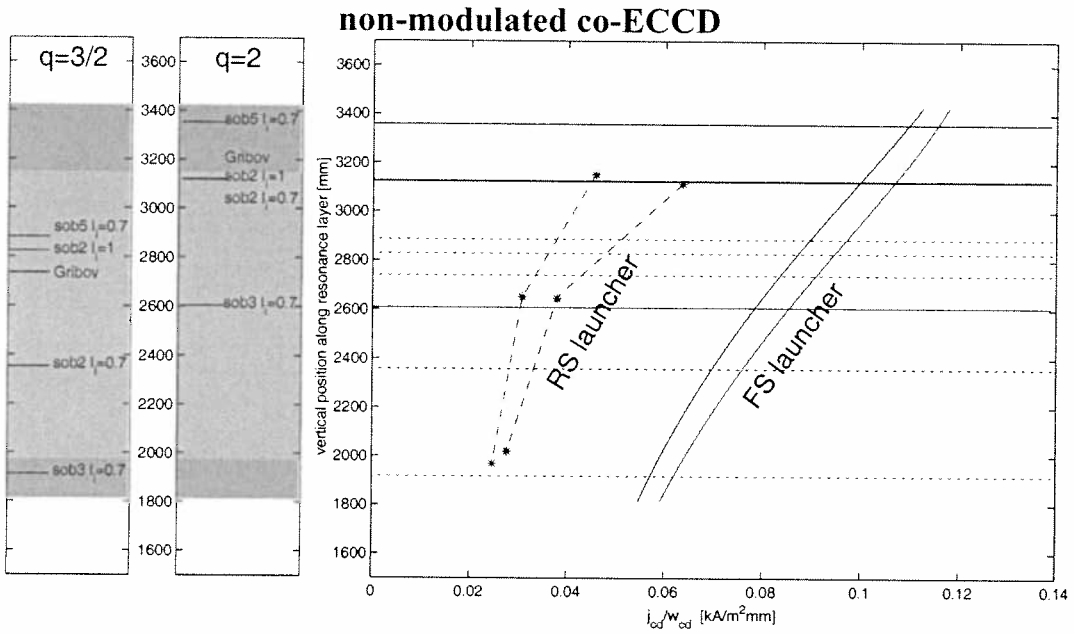

Figure 10a The NTM stabilization figure of merit (non-modulated co-ECCD) for the RS (dashed lines) and FS (solid lines) launcher can be estimated using the free space beam size at the resonance (figure 8) and the relation between the free space beam width and the peak driven current density and deposition width (figure 9). The FS launcher has double the efficiency for stabilizing the NTMs over a wider range. The vertical location of the q=2 (solid horizontal lines) and q=3/2 (dashed horizontal lines) along the resonance layer is given for the relevant ITER equilibrium.

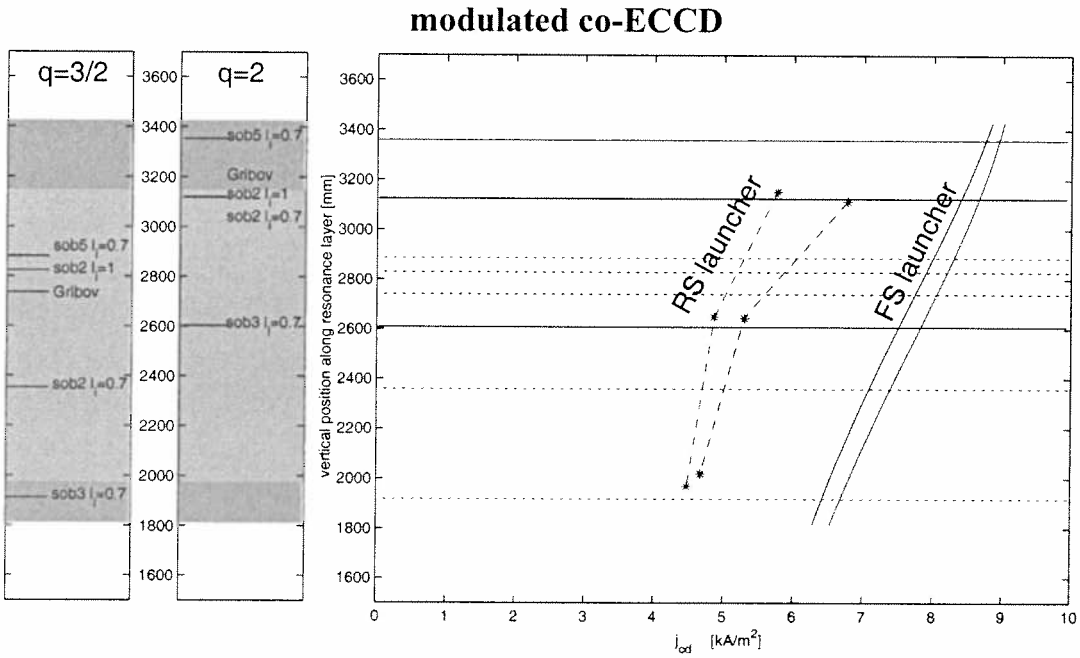

Figure 10b The NTM stabilization figure of merit (modulated co-ECCD) for the RS (dashed lines) and FS (solid lines) launcher can be estimated using the free space beam size at the resonance (figure 8) and the relation between the free space beam width and the peak driven current density and deposition width (figure 9). The FS launcher has 40%increase in efficiency for stabilizing the NTMs over a wider range. The vertical location of the q=2 (solid horizontal lines) and q=3/2 (dashed horizontal lines) along the resonance layer is given for the relevant ITER equilibrium.

The front shield opening for the FS launcher is approximately 330mm horizontal and 430mm vertical, which corresponds to 330mm and 650mm, respectively, for the RS launcher. The surface area of the opening is about 2/3 smaller for the FS launcher compared to the RS launcher. The reduced size of the opening can be attributed to the location of the rotation points of the upper and lower launchers, which are much closer to the front panel for the FS launcher.

The waveguide "line-of-sight" corresponds to the path along the axis of the last leg of the waveguide toward the plasma. The neutron streaming will decrease if the waveguide views further off axis. In the case of the FS launcher, the viewing angle has been arranged so that the waveguide does not "see" the plasma, but aims above it as shown in figure 1. However, the waveguide in the RS launcher are either parallel or tilted downward relative to the port axis, resulting in a potentially larger increase of the neutrons streaming down the waveguide.

The gap between the back plate of the front shield and the focusing mirror has been increased to ~60mm from the previous design. The added space allows a region for a support structure to hold the mirror in place and additional shielding material behind the mirror. The steering mirror is recessed ≥120mm behind the front panel. The increased distance will reduce the sputtering rate from the incident charge exchanged neutrals coming from the plasma.

The empty space not occupied by the RF beam will be filled with shielding material. The volume occupied by the beam and launcher components will reduce the effective shielding capabilities of the port plug. It is difficult to estimate this volume at this present stage in the FS design. It appears that the increased spacing from the waveguide to the focusing mirror, in addition to the larger waveguide diameter will decrease the amount of shielding material in the port relative to the RS design. The reduction of the shielding material will be quantized in the future.

6) Alternative scenarios

In addition to the already mentioned flexibility in the FS design in using either 45mm or 63.5mm waveguide and using either the double miter bend or a straight waveguide section, there are a few added alternative designs that may be advantageous for ITER. These are briefly described below.

6.1) Untouched blanket shield

The current FS design was created using similar design restrictions as used for the RS launcher. This includes removing a small section of the lower blanket module[1], permitting passage of the microwave beam from the lower launcher when heating the inner most q=3/2 surface. The FS launcher can be redesigned to avoid the conflict with the lower blanket region as shown in figure 11.

1. As presented in the CATIA FZK model of: v1_19_05_04.zip

Figure 11 The FS launcher can be designed such that there is no interference with the lower blanket shield. Such a configuration will decrease the efficiency in stabilizing the NTMs, while maintaining a similar steering range as the current FS launcher design.

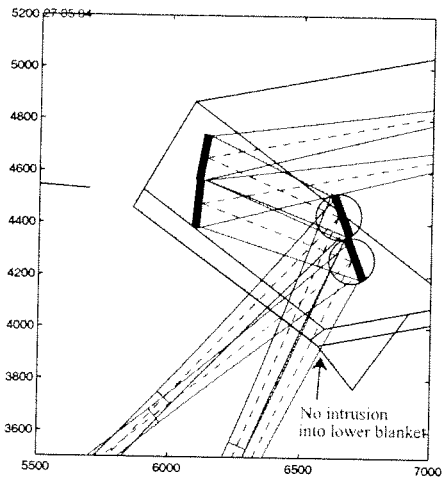

6.2) NTM stabilization + ELM destabilization

Counter-ECCD near the edge has recently been used successfully on ASDEX-Upgrade to control the ELM frequency. The present FS design uses only three of the four upper ports reserved on ITER for NTM stabilization. If all ports are used, then the lower row of launchers can be reserved for NTM stabilization, while the upper row for another purpose such as ELM destabilization (note: this is a similar port allocation as the dedicated launcher approach of the RS launcher) as shown in figure 12. Note: the mirror configuration is far from optimized, the drawing only illustrates the capability of a dual purpose upper launcher. Such an approach leaves the launcher design flexible to accommodate possible advances in the coming future.

Figure 12 Using the dedicated line approach of the RS launcher, the FS upper and lower launchers could be designed to expand the flexibility of the upper launcher beyond the realm of only NYM stabilization. For example, in this case the upper launcher is used to destabilize ELMs by delivering counter-ECCD on the plasma edge, while the lower launcher maintains a similar steering range for NTM stabilization. In both cases the steering mirror size can be increased, which will reduce the free space beam size at the resonance layer.

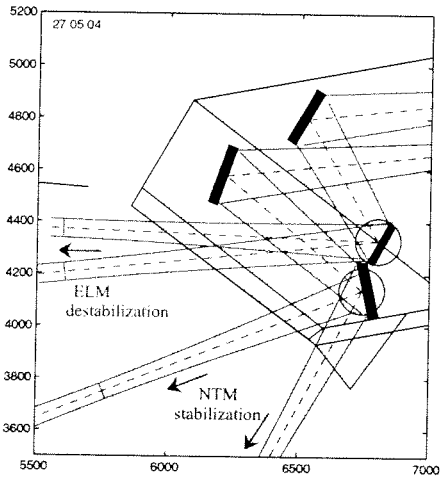

6.3) Hybrid sweeping range

The hybrid launcher design limits the angular range of the lower launchers over the region of the q=2 surfaces, see figure 13, which permits an increase in the vertical extent of the mirrors and a larger beam spot size. The larger beam spot size is used to project the beam waist further into the plasma reducing the deposition width for co-ECCD on the q=2 surface. Full power can be applied on all q=2 (and a majority of the q=3/2) equilibrium positions (only the upper launcher has access to the q=3/2 surface in the sob7, l_i=0.7 equilibrium).

Figure 13 The hybrid launcher reduces the scanning range of the lower launchers in exchange for an increased size of the steering mirror. In exchange of the reduced scanning range both upper and lower launchers have a narrower free space beam width along the resonance layer, increasing the NTM stabilization efficiency over the various vertical locations of the q=2 surfaces. The scanning range of the upper launcher is maintained for all q=3/2 NTM stabilization.

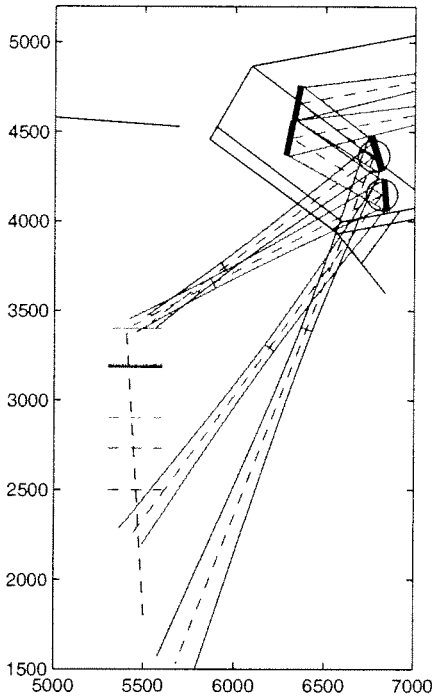

7) Conclusion

The FS launcher study has produced a two mirror launcher design which focuses the RF beam far into the plasma. The first mirror is focusing-fixed while the second is flat and rotatable. The design is compatible with either 45mm or 63.5mm waveguide. The flexibility of the FS launcher concept offers alternative designs, which avoid interference with the lower blanket shield, increase the NTM stabilization efficiency (at the cost of a reduced steering range) or expand the role of the upper launcher (for example ELM destabilization). The current design still needs to be further optimized. In particular, the spread in toroidal injection angle between each two beam set needs to be reduced by optimizing the relative poloidal injection angles. Also, the steering mirror size can be increased to further reduce the beam spot size at the resonance.

The purpose of the study was to determine if the FS launcher could offer an improved performance relative to the RS launcher. The current design offers a steering range has been increased by $\geq$ 40% relative to the RS launcher (April 2004 design). Also the NTM stabilization efficiency is increased by a factor of $\geq$2 (1.4) over the complete steering range for non-modulated (modulated) co-ECCD injection available relative to the RS launcher. The FS mirror arrangement may also improve the neutron shielding capabilities of the upper port since the front panel opening is reduced by 30% and the introduction of the optional miter bend pair should significantly reduce the neutron streaming down the waveguide. In addition,.

8) Acknowledgements

The authors would like to thank D. Farina, S. Nowark and G. Ramponi for providing the beam tracing calculations used in this report. O. Sauter provided helpful support in characterizing the NTM stabilization efficiency figure of merit. Also, S. Alberti, T.P. Goodman, J.-P. Hogge, D. Fasel, and L. Porte are to be acknowledged for the indirect participation via numerous discussions concerning the design of the FS launcher. This work was supported in part by the Swiss National Science Foundation.

Appendix A

Re-Investigation of a Front Steering Launcher on ITER's Upper port

M.A. Henderson, R. Chavan and F. Sanchez

19.03.04

CRPP has offered to launch a study that reconsiders the implementation of a front steering (FS) ECRH launcher on ITER's upper port. The preliminary objective is to redesign a FS launcher with a steering range of ± 12° and a beam spot size of ≤80mm after 3.0m from the steering mirror. This document gives a brief perspective on the motivation, optimization parameters, goals and scheduling of the proposed preliminary design study. The outline of this document is as follows:

1. Motivation

The planned ECRH system for ITER is being designed based on an extrapolation from today's current physics understanding to tomorrow's application on ITER. Unfortunately, our understanding is limited, and coupled with the extrapolation from existing machines to ITER, leaves a potentially wide range of required launching parameters for the upper launcher. In the past ten years significant advances in the application of ECRH and ECCD have been made, which includes the use of co-ECCD for NTM stabilization (Zohm et al, Nucl. Fusion 39 (1999) 577). The next ten years may prove to be as fruitful as the past, leading to even more advances in the application of ECRH and ECCD, and offering an even wider spectrum for the application of the upper launcher on ITER. Today's design of the upper launcher should attempt to offer the largest range of steering angles and the highest power density for optimizing ITER's performance, and at the same time remain flexible to adapt to the evolving use of ECRH and ECCD in tokamak physics.

A front steering launcher may offer an increased flexibility with a greater steering range and higher power density over the present remote steering (RS) launcher. The RS launcher has advantages over the FS launcher; the most obvious is the removal of the steering mechanism from near the plasma boundary to the outer surface of the neutron shield, which is essential for a burning reactor. However, the RS launcher is limited in angular range and the transmission efficiency decreases as the injection angle increases from the center angle. It is unfortunate that the RS launcher application on ITER will operate principally in the non-optimal case of ≥ ± 6°. If a wider steering angle of >12° is required for NTM stabilization on ITER or if the power density at resonance surface is not sufficiently high to fully stabilize the NTMs, then the usefulness of RS launcher in fusion application along with ECCD may be brought to question. Ideally, the RS launcher should be held in reserve for optimal application once the required ECCD parameters are better understood.

The technological complexities of the front steering launcher with ±12.5° of steering range are nearly (if not already) solved for the equatorial launcher (Takahashi et al, FED 66-68 (2003) 473), where the neutron and thermal fluxes are higher than for the upper launcher. The appli-

cation of a FS launcher in the region of the highest neutron and thermal fluxes, while installing a RS launcher in the region with lower fluxes, appears to the authors as an inverted logic. Since the physics demands of the equatorial launcher require a large steering range, essentially "forcing" the use of a FS launcher, why not apply the same technology to the upper port (where neutron and thermal fluxes are lower), and increase the steering range and power density at the q=2 & 3/2 resonance? This could offer an improved flexibility in the ECRH system for the success of ITER.
In addition, due to the recent increased range in required steering angles, the port opening on the RS launcher has increased beyond that which is required for a FS launcher. The larger port opening decreases the shielding of neutrons streaming in the direction around the transition zone from the equatorial port to the vessel wall. Of particular concern is to maximize the shielding of the upper poloidal field coil (PF2).
It is with these thoughts in mind that the authors wish to explore in greater depth than previously, the capabilities of a FS launcher for ITER's upper port. Our goal is to determine if the FS launcher can offer an increased steering range and a higher power density at the resonance surface relative to the RS launcher for the benefit of the ITER performance.

2. Parameters of Optimization

As can be understood from the motivation, the principle parameters of optimization will be to maximize the power density at the q=2 and 3/2 resonance surfaces and provide the widest range of steering angles possible. These two parameters are in conflict; the largest steering angle would require a small spot size on the steering mirror, which results in a beam with a larger divergence angle and lower power density at the resonance. In contrast, a large beam waist (near the steerable mirror) would maximize the power density at the resonance, but reduces significantly the available space for the larger mirror needed for steering the beam. Along with trying to obtain an optimum between these two parameters, several other parameters will be considered in designing an optimum FS launcher, are listed below:

- Maximize the power density at the resonance location (spot size < 80mm). The optimization will minimize the power density on the q=2 surface (more critical than the q=3/2 surface for NTM stabilization).
- Maximize the steering range ($\Delta a \geq 12^{\circ}$)
- Minimize opening at the first wall.
- Minimize the poloidal cross section to reduce EM forces on steering mirror during disruptions.
- Maximize spot size on steering mirror to reduce peak power density.
- Minimize losses in launcher to maximize delivered power at the resonance.
- Maximize the independent steering of beams (two beams incident on one steering mirror).
- Maximize the neutron shielding capability regarding the upper poloidal field coil (PF2).

3. Design Characteristics

The following list includes the preliminary characteristics that are to be considered for the FS launcher:

• A launcher design with 8 entry beams of 1.0MW and a second design with 4 entry beams of 2.0MW. If time permits, we will also investigate a launcher with 8 entry beams of 2.0MW.

• One fixed focusing mirror and one steerable flat mirror (if possible).

• Compatibility with both 63.5mm and 45mm circular HE11 corrugated waveguide. Note: the power density of 2MW in 45mm waveguide is equivalent to what has already been achieved with 1MW in 31.75mm waveguide, so the application of the 45mm waveguide is not a limitation.

• Two separate FS designs will be developed using the steering mechanisms from the Japanese team (Takahashi et al, FED 66-68 (2003) 473) and R. Chavan's design (Support of the Design of the ITER EC H&CD System: Design of the Upper Port Launcher)

• Keep each waveguide axis parallel to the port axis and at sufficient distance for the introduction of gate valve and CVD window at port entry.

•waveguides are to be in a 4 x 2 array (if possible).

• Maintain a 20 mm clearance around wall of port plug and front shield (if possible) in order to ensure the maximum mechanical stiffness of the plug's outer shell.

• Work around the base design of b=20° and a0 centered half way between the q=3/2 and 2 flux surfaces for each steering mirror (these angles can easily be modified as the physics requirements develop).

• We will assume that maximizing the power density at the q=2 resonance will also correspond to the maximum EC current density in Y.

• All beams will be steerable in the poloidal direction to insure a complete 8 beam super positioning that maximizes the current density in Y.

• The toroidal injection angle of all beams will be within 18°<b<21° (if possible). Recent ray tracing and current drive calculations indicate that the optimum current density is obtained for b=20° (D.Farina et al, "ECWGB: a beam tracing code for EC heating and current drive", IFP-CNR Internal report FP 03/6, October 2003). The calculations also indicate that nearly equivalent current densities can be obtained with 18°<b<21°. A small spread in toroidal angle helps in concentrating the beams on the steerable mirror, while maintaining a complete 8 beam super positioning at the resonance in Y.

• Spot size on mirrors will be 3.5w (for comparison with RS design).

• Design an increased steering angle range (± 20°) while sacrificing power density at the resonance.

• Design a maximized power density at the resonance with a limited steering range (± 8°).

Note: this last two designs will provide the physicists with a relation between the increased steering angles and increased power densities.

• Characterize beams for ray tracing analysis.

4. Schedule

A complete report of the design activities of the FS launcher will be delivered on or before April 16th. The beam optics, mirror sizes, 3D drawings, and all other information that will be necessary for evaluating the FS launcher will be provided in the above report. On March 26th and April 4th a status report will be assembled summarizing the previous weeks activities. CRPP would solicit comments on these status reports in helping to guide the design in a direction optimal for the ITER program.

Appendix B

FS Launcher Status (22.03.04)

A preliminary un-optimized launcher design has been created for eight 1.0MW beams per port and a similar design for four 2.0MW beams per port. The main goal at this point is to find a quasi-optical solution for launching the eight (or four) beams with a relatively large beam waist located near the opening of the upper port. The preliminary solution will be presented in this report. The next step will be to incorporate the design in Catia and then attempt to optimize the launcher design considering available space with in the port and reducing the spot size at the q=2 surface as small as possible. The present design has four beams incident on one steering mirror (for the 1.0MW beams). This removes the independent control of each beam, but allows a large beam spot size on the steering mirrors and a low beam divergence reducing the ultimate spot size at the resonance surface. Spot size after 3.0m of both launchers is $w \leq 76mm$.

Steering mirror structure:
The mechanism for the steering mirror (SM) uses a hybrid of the system proposed by R. Chavan (Support of the Design of the ITER EC H&CD System: Design of the Upper Port Launcher). The length has been decreased by 33% while increasing the diameter by 25% maintaining the same rotation capabilities (+/- 10°).

Four Beam - 2.0MW Launcher:

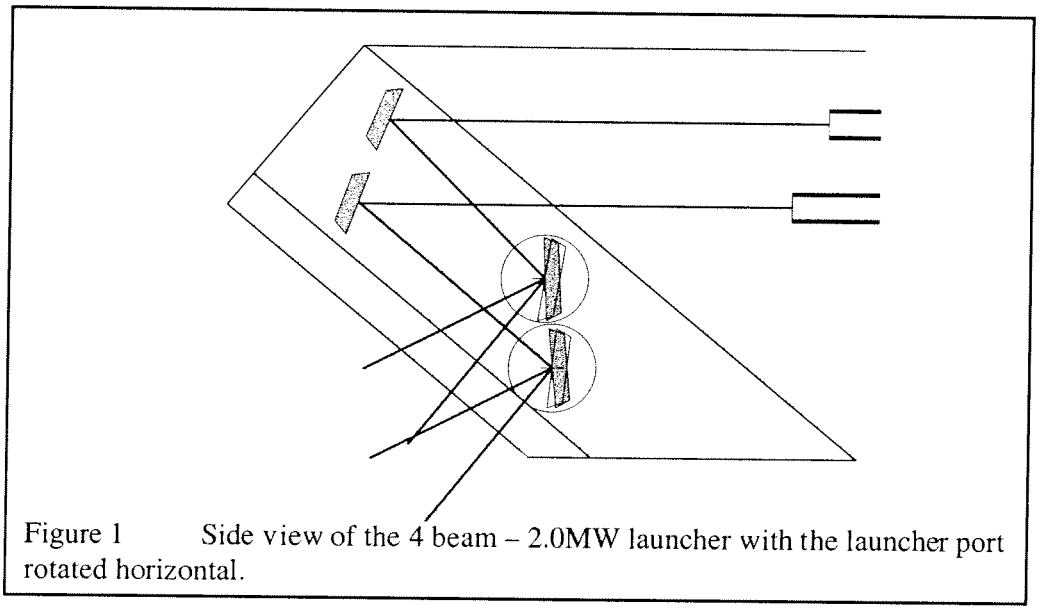

Figure 1 Side view of the 4 beam – 2.0MW launcher with the launcher port rotated horizontal.

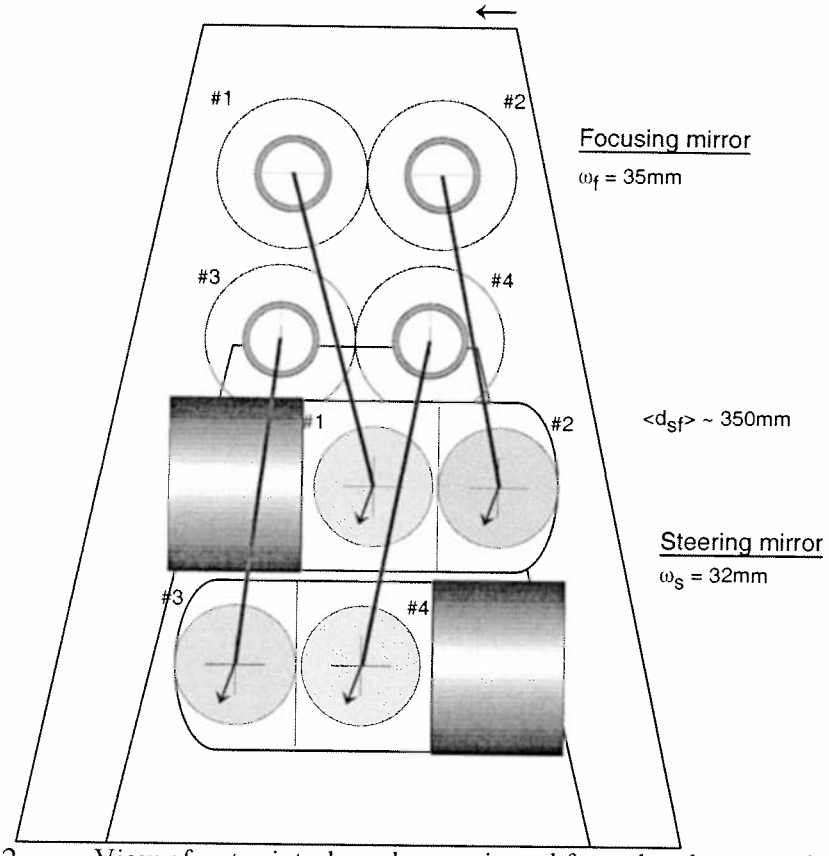

Figure 2 View of entry into launcher as viewed from the plasma and looking along port axis. Beam path is in blue.

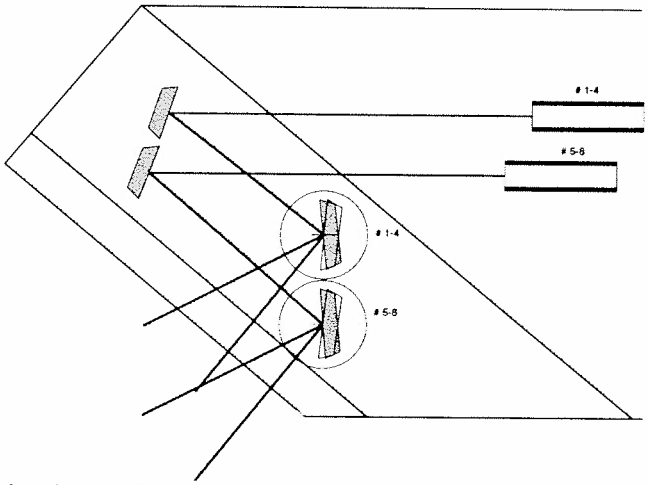

Figure 3 Side view of 1.0MW launcher. Four beams are overlayed in a given horizontal plane.

The 2.0 MW launcher will be present first, it is simpler in design and is easier to describe than the 1.0MW launcher. A side view of the launcher is shown in figure 1, the port has been

rotated so that the port axis is horizontal in the figure and the plasma is to the left. The beams are projected from the waveguides (upper right corner), which enter from the right, and is incident on a focusing mirror (one mirror for each beam). The beams are projected downward to the steering mirror and then into the plasma (b=20°). The spot sizes on the mirrors are large with the peak power density on focusing mirror is equivalent to a 1.0MW beam with w=24.7mm. The power density on the steering mirror is equivalent to a 1.0MW beam with w=22.6mm (reducing the steering angle to +/- 8° will allow an increase in the beam spot size on the mirror to 34.9mm, equivalent to 25mm for 1MW)). A front view looking into the port along the axis is given in figure 2.

Eight Beam - 1.0MW Launcher:

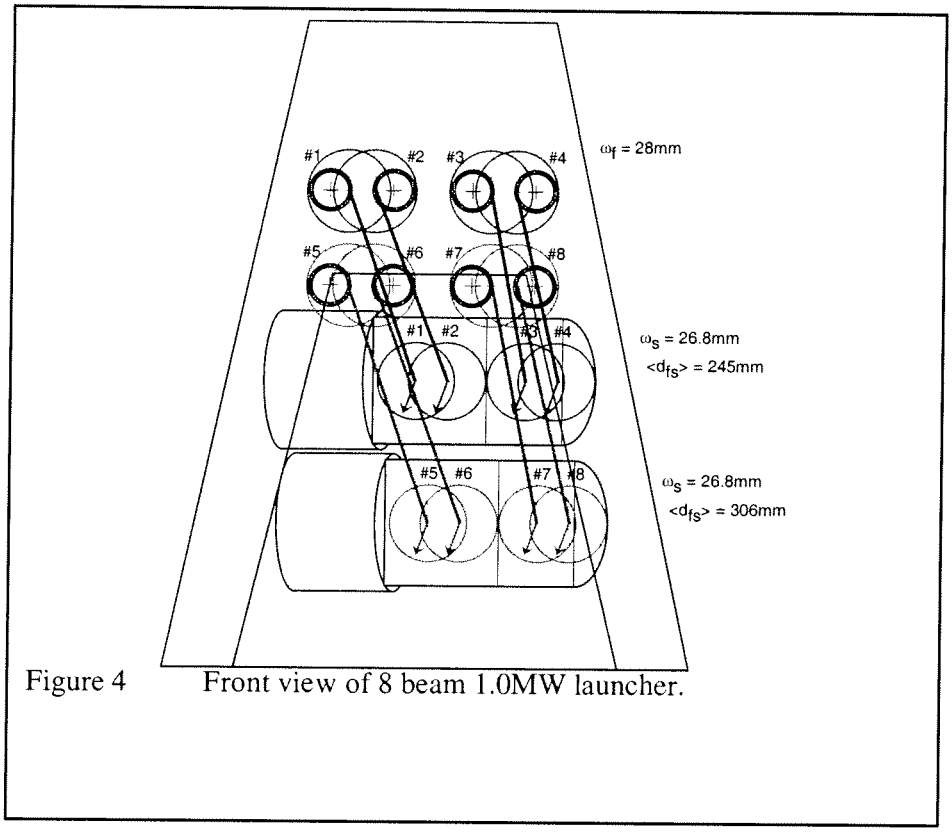

Figure 4 Front view of 8 beam 1.0MW launcher.

A similar configuration of waveguide and mirrors is used as in the four beam 2.0MW. However, sets two beams are projected onto a focusing mirror. The waveguide will be slightly tilted so that the output beams are parallel and offset by 15.4mm, maximum power density is equivalent to one beam with w=25mm).

Next Step

1. Minimize spot size at q=2 surface (need to determine distance from the center of each mirror to the q=2 surface).
2. Increase spot size on steering mirror for 4 beam – 2.0MW launcher (keep maximum power density less than equivalent to 1.0MW with w=25mm). Use only +/- 8° steering range for comparison with RS launcher.
3. Characterize beam (beam waist size, location, etc.) for ray tracing codes.
4. Create Catia drawing of launcher.

Appendix C

FS Launcher Status Report #2 (02.04.04)

Introduction

The design work since the last status report (SR#1 of 22.03.04) has concentrated on a two mirror system as shown in figure 1. This mirror arrangement seems the most promising for maximizing the steering range, power density at the resonance as well as maintain an 8 beam input for each launcher port. The first mirror is a focusing mirror with two beams incident on the surface. Each beam is displaced by a distance $\pm\Delta_f$ in the toroidal direction (perpendicular to the page of figure 1) relative to the mirror center. Working in the constraints defined by the walls of the blanket shield, the size of the mirrors were increased in order to decrease the peak power density on the steering mirror surface. Then a focal length of the focusing mirror was chosen to minimize the spot size of the projected beam at the q=2 resonance. Once the beam optics were defined, a preliminary check of the position and dimensions of the steering mirror was performed. The steering mirror and projected beam from the port shield was included in the CATIA drawing of the ITER upper port. This status report will describe in more detail the above steps and outline the next steps to be taken.

Optimizing the beam spot size on the steering mirror

The main constraint in designing the FS launcher is the toroidal width of the blanket shield region of the port. The port width in this region is ~430mm and in this space must fit a mirror large enough to reflect four incident beams plus the steering mechanism outlined by Rene Chavan (see: Support of the Design of the ITER EC H&CD System: Design of the Upper Port launcher). The steering mechanism (SM) is cylindrical in shape and was originally 180mm long and 140mm in diameter. The same flexibility (±10° mirror rotation) could be maintained by increasing the diameter (to 170mm) and decreasing the length (to 125mm), which increases the available space for the mirrors, i.e. a larger beam spot size on the mirror. A sketch of the port as seen from the plasma (looking along the port axis) is shown in figure 2. A mirror of 280mm in toroidal extent can fit within the remaining space.

The current FS design splits each steering mirror in half with two partially overlapping beams incident on each half section (offset from the half section center by $\pm\Delta_s$). Each half section is tilted about a vertical axis to direct the two beams with a toroidal injection angle of β~20°. The degree of tilt depends on the beam geometry and will be different for the two half mirror sections. The center of each half mirror is positioned along the axis of the SM. A small vertical ridge is created in the center of the mirror. The partial overlap of the two beams on each mirror half reduces the toroidal extent of the mirror without significantly increasing the peak power density, see figure 3. Note the mirror diameter size is taken as 3.5ω (in E-field) throughout this report (for direct comparison with the FS launcher design).

The absorbed power on the mirror surface is given by (W/mm^2):

$$\left(\frac{dP}{dA}\right)_{max} = \frac{2P_0P_{abs}}{\pi\omega_s^2} \qquad \text{E-plane polarization}$$

$$\left(\frac{dP}{dA}\right)_{max} = \frac{2P_0P_{abs}}{\pi\omega_s^2}\cos^2(\theta_i) \qquad \text{H-plane polarization}$$

where P_0 is the beam's incident power, P_{abs} is the absorbed power fraction, ω_s is the beam spot size on the mirror and θ_i is the incident angle. The absorbed power fraction depends on the material, temperature, impurity content, etc. This report will use a value of 0.00268, which is twice the value for copper at 200°C. Doubling the absorbed power fraction is an approximation which takes into account higher temperatures above 200°C and impurity effects. This value is slightly lower than the absorbed power fraction used for the equatorial launcher, 0.00347 (K. Takahashi et al, FED **56-57** (2001) 587-592). However, the specific value is not critical for the comparative study between the RS and FS launchers. In this report, the incident polarization is assumed to be circular as a close approximation of what will be used for co-ECCD injection on ITER. Circular polarization will have half the power in both E and H-plane (with a 90° phase shift between the two polarizations), so an average of the above two equations will be used throughout this text.

An optimum in offset distance, Δ_s, exists that minimizes the peak power density on the steering mirror, this can be obtained by calculating the peak power density while scanning the beam spot size incident on the mirror and using the following relationship:

$$3.5\omega_S - 2\Delta_S = 140\text{mm}$$

where ω_s is the spot size on the mirror, the width of the mirror is set at 140mm. A local minimum in the peak power density is observed for a spot size of 30mm and an offset distance of 17.5mm, as shown in figure 4 (P_0 ~1.5MW). These values were used in the double beam plot of figure 3, where the peak total power density is 8.34% above that of an individual beam. The power density on the steering mirror is of principle concern, since the spot sizes and beam separation distances are larger for the focusing mirror.

The resulting peak power densities on the plasma facing mirrors of both launchers are given by:

$$\left(\frac{dP}{dA}\right)_{max}[W/cm^2] = \frac{3P_0(0.268)}{2\pi\omega_s^2} \qquad \text{RS launcher}$$

$$\left(\frac{dP}{dA}\right)_{max}[W/cm^2] = 1.0834 \bullet \frac{3P_0(0.268)}{2\pi\omega_s^2} \qquad \text{FS launcher}$$

for both launchers θ_i=45° was used. The spot sizes on the plasma facing mirror for the FS launcher are larger resulting in a lower peak power density as shown in figure 5. The spot sizes used were ω_{Rl}=16.8mm (lower RS mirror, solid red line), ω_{Ru}=18.4mm (upper RS mirror, dashed red line) and ω_{FS}=30.0mm (steering FS mirror, blue line). The larger spot size on the FS mirrors significantly decrease the maximum power density and offer ~2.0MW operation based on the power density limitation of 300W/cm^2 (R. Heidinger, 26 Nov. 2003). The power densities on both the upper and lower mirrors of the RS launcher appear to be limited (to ≤750kW incidence power) for the same maximum power density. The absorbed power fraction used in this report is lower than the 0.5%, which was used to estimate a 1240W/cm^2 peak power density for 2.0MW incidence power (First intermediate report on Upper Launcher

design activities, EFDA Task TW3-TPHE-ECHULA and B, page 29)Note: temperature effects on the absorbed power fraction are not accounted for in figure 5 .

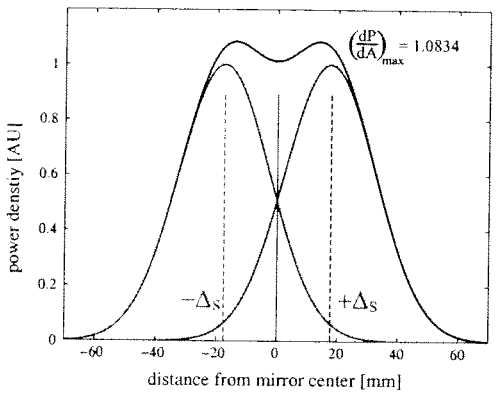

Figure 3 The partially overlapping beams are offset by a distance $\pm\Delta_S$, which reduces the size of the steering mirror, while only slightly increasing the maximum power density on the mirror.

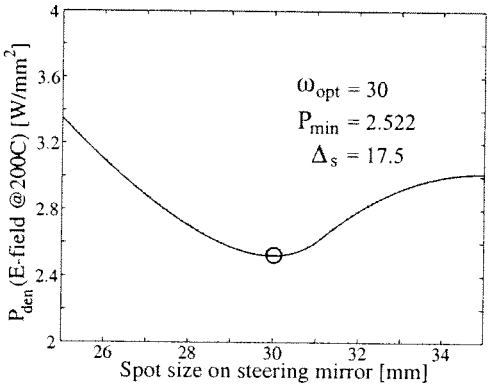

Figure 4 A local minimum in peak power density occurs when ω_s=30mm and Δ_s=17.5mm for a mirror of toroidal width of 140m.

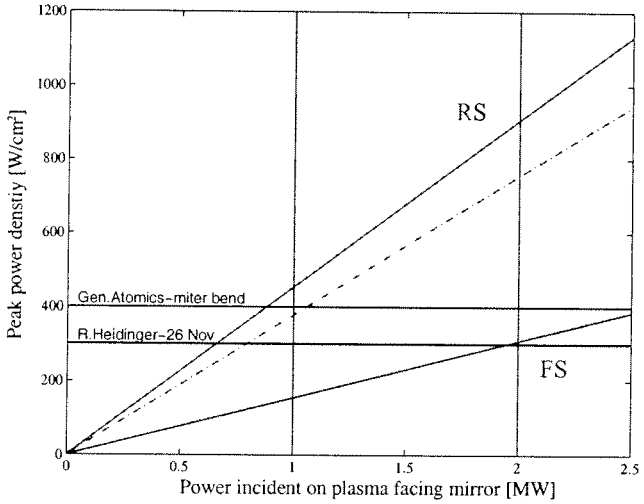

Figure 5 Peak power density on the lower (dashed red), and upper (solid red) mirrors of the RS launcher compared to the peak power density of the FS steering mirror (blue line). The horizontal lines correspond to the peak power limitation of ITER (R. Heidinger 26 Nov.) and that used by General Atomics on their miter bends.

Power density on q=2 surface

For minimizing the power density at the q=2 resonance surface, the beam waist should not be too small (avoid large divergence angles) and should be projected far into the plasma. A large spot size is required on the focusing mirror, in order to project the beam waist any significant distances. Increasing the distance from the waveguide to the focusing mirror, lets the beam expand. In this respect the RS launcher is handicaped, the beam leaving the square waveguide has a small beam waist and a wide spread in launching angle. The focusing mirror would have to be extremely large to "catch" the exiting beam at all launching angles, if the beam was allowed to expand. Thus the mirror must be relatively close to the waveguide, limiting the spot size on the mirror and, in turn, the projection of the beam waist into the plasma.

However, for the FS launcher, the beam exiting the waveguide can expand to a large size, and then refocus the beam such that the beam waist is over 1.0m away. The focusing mirror's focal length is chosen to minimize the spot size at the q=2 resonance location using the following equations:

$$\omega_S = \omega_0 \sqrt{1+\left(\frac{2d_{s0}}{k\omega_0^2}\right)^2}$$

$$\omega_{r2} = \omega_0 \sqrt{1+\left(\frac{2d_{0r2}}{k\omega_0^2}\right)^2}$$

$$d_{sr2} = d_{s0} + d_{0r2}$$

where ω_s and ω_{r2} are the spot sizes on the steering mirror (30mm) and q=2 resonance (to be minimized), ω_0 is the beam waist (fit variable), d_{s0} is the distance from the steering mirror to the beam waist, d_{0r2} is the distance from the beam waist to the q=2 resoance. All parameters are on the plasma side of the focusing mirror. The distance d_{sr2} (distance from steering mirror to q=2 resonance) depends on the ITER equilibrium chosen, this report used 1420mm for the lower mirrors and 1520mm for the upper mirrors.

The resulting spot size on the q=2 surface is significantly smaller than what can be achieved with the RS launcher, as shown in figure 7. The beam characteristics for the RS launcher were taken from T. Verhoeven's presentation of 26 Nov. 2003 and the position of the q=2 and 3/2 surfaces from D. Farina's presentation of the same date. The FS launcher beam is from the optimization process described above. The power density relative to the RS launcher is increased significantly at the resonance location of the q=2 and 3/2 flux surfaces:

Table 1: Averaged Resonance spot size comparison

	$<\omega_{RS}>$	$<\omega_{FS}>$	$(<\omega_{RS}/\omega_{FS}.)^2$
q=2	47.2	25.1	3.5
q=3/2	59.6	33.1	3.2

The optimization procedure performed had a larger d_{sr2} than required for the ITER equilibrium used in the above comparison. Repeating the same optimization process for the above equilibrium would yield $\omega_{FS}(q=2) < 23$mm. Ray tracing calculations using the above beam characteristics are now in progress for comparison with the RS launcher.

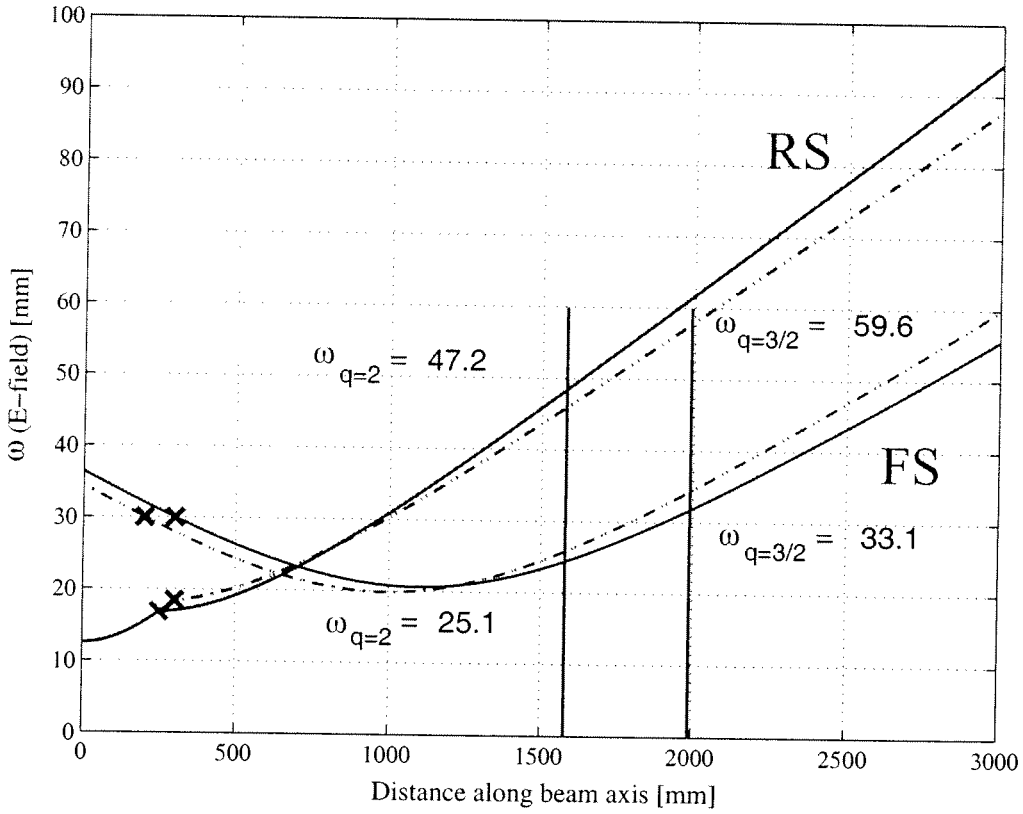

Figure 7 Beam waist of the RS (red) and FS (blue) launchers (upper launcher dashed, lower launcher solid) as a function of the distance from the end of the RS rectangular waveguide. The position of the last mirror for both launchers are at the 'X', note the distance of the horizontal axis is shifted for the FS launcher according to the distance from the last mirror to the q=2 resonance surface. The vertical green bars correspond to the position of the q=2 and 3/2 surfaces.

CATIA Drawing

The beam from the steering mirror to the resonance surface was included in the ITER upper port as a preliminary check of the mirror size. There was a small conflict with the upper steering mirror, which touches the wall of the blanket shield near beam #4 (see figure 2). However, the conflict can easily be avoided by displacing the whole mirror assembly to the left (as shown in figure 2) a few millimeters, still leaving enough space for the SM.

Next steps

The next steps we will pursue are:

1) Characterize the full beam trajectory from the waveguide to the plasma.

2) Design alternative launcher with larger mirrors or larger steering range

3) Continue work on modifying the SM.

4) Begin work on the waveguide at the entrance to the launcher port.

5) Incorporate all elements in CATIA V5R12SP6.

6) Determine opening size on the front plate.

This will be the last status report. The next report will be a final report, which is to be delivered at the conclusion of this study in aproximately three weeks time.

Appendix D

Power Density on plasma facing mirror

The intensity of a gaussian beam is given by:

$$I(r) = \frac{2P_0}{\pi\omega_m^2} e^{-\left[\frac{2r^2}{\omega_m^2}\right]}$$

where P_0 is the beam's incident power and ω_m is the beam spot size on the mirror in E-field. The peak power density on the mirror surface is at the center of the beam, or:

$$\left.\frac{dP}{dA}\right|_{peak} = I(r=0)$$

The peak absorbed power density (in W/mm^2) of a gaussian beam with an incidence angle of θ_i on a mirror is given by:

$$\left.\frac{dP}{dA}\right|_{peak-\Omega} = \frac{2P_0\eta_\Omega}{\pi\omega_m^2}\cos(\theta_i)$$

The absorbed power fraction, η_Ω, is given by :

$$\eta_{\Omega-E} = 4s\sqrt{\frac{\varepsilon_0\pi\mu_0 f}{\sigma}}\frac{1}{\cos(\theta_i)} \qquad \textbf{E-plane}$$

$$\eta_{\Omega-H} = 4s\sqrt{\frac{\varepsilon_0\pi\mu_0 f}{\sigma}}\cos(\theta_i) \qquad \textbf{H-plane}$$

where s is the surface roughness factor generally taken as 2, ε_0 and μ_0 are the permittivity and permeability of free space, f is the frequency and σ is the mirror's conductivity. Using twice the Cu resistance at 200°C, which compensates for an increased temperature and surface impurities, the absorbed power fraction (with θ_i=0°) is:

$$4s\sqrt{\frac{\varepsilon_0\pi\mu_0 f}{\sigma}} \cong 0.0035$$

The value 0.0035 is derived from K.Takahashi et al, FED 56-57 (2001) 587 and is consistent with the equvalent value from GA of 0.0033. The injected ECRH beam for the upper launcher will be O1 and co-ECCD, which requires nearly circular polarization for optimum coupling. Using circular polarization, which is an over estimate since more power will be in H-plane than E-plane polarization, the maximum power density is taken as an average of the E-plane and H-plane polarization, or

$$\left.\frac{dP}{dA}\right|_{peak-\Omega} = \frac{2P_0\frac{(\eta_{\Omega-E}+\eta_{\Omega-H})}{2}}{\pi\omega_m^2}\cos(\theta_i) = \frac{0.0035P_0}{\pi\omega_m^2}\left(1+\cos^2(\theta_i)\right)$$

There is a physical limit on the maximum peak absorbed power density (dP/dA_{max}) on the mirror surface depending on the material chosen, surface temperature, cooling system, etc. The above equation can be used to determine the minimum beam spot size on a mirror in relation dP/dA_{max}.:

$$\omega_{m-min} \geq \sqrt{\frac{0.0035P_0\left(1+\cos^2(\theta_i)\right)}{\pi \left.\frac{dP}{dA}\right|_{max}}}$$

The peak power density has been estimated as 3.0W/mm^2 (R. Heidinger 26 Nov. 2003), this value can be increased slightly to 3.2W/mm^2. K. Takahashi [FED 66-68 (2003) 473] calculated for the equatorial FS launcher that the temperature would increase to 393°C for a 1.0MW beam with ω_m=23mm (E-field). There were three sources of power included in his calculation: 3.17W/mm^2 from the RF beam, 2.0W/mm^2 from plasma thermal radiation and 1W/cm^3 from nuclear radiation. Using the 3.2W/mm^2 limit, a minimum "allowed" spot size can be plotted as a function of incidence angle for various injected powers.

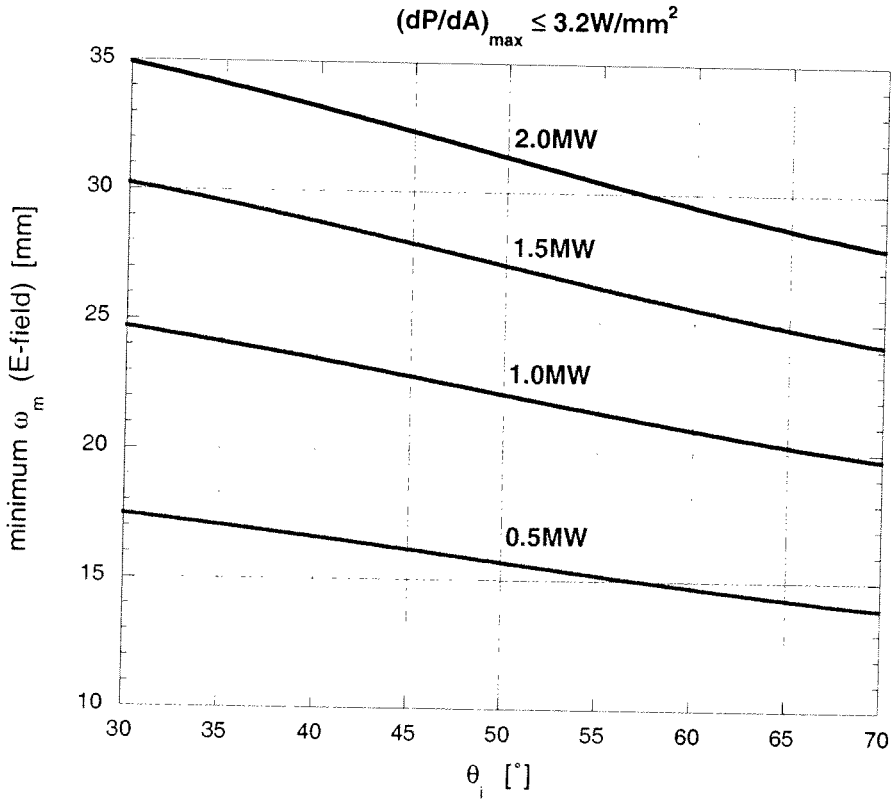

This implies that for 2.0MW injection the spot size on the plasma facing mirror needs to be around 33mm, assuming $\theta_i \geq 40°$. The peak power density can be increased using improved cooling techniques. For example, the gyrotron cavity uses hypervapotron cooling that permit peak power densities of the order of 20W/mm^2, which would be sufficient for the current RS mirror design. However, this peak power density is valid only in the cavity region of the

gyrotron, which is very localized in volume and in a fairly controlled enviornment. The hypervapotron technique is also applied in the cooling the gyrotron collector (which would be comparable application to the RS launcher mirror), and the peak power density is limited to less than $5W/mm^2$.

The Maximum injected power can be calculated as a function of the incidence angle for a given spot sizes using:

$$P_{0-max} = \frac{\pi\omega_{m-min}^2 \left.\frac{dP}{dA}\right|_{max}}{0.0035\left(1+\cos^2(\theta_i)\right)}$$

Applying this to the RS (ω_m=16.8mm & 18.4mm) and the FS (ω_m=30mm spot size) launchers yields the following:

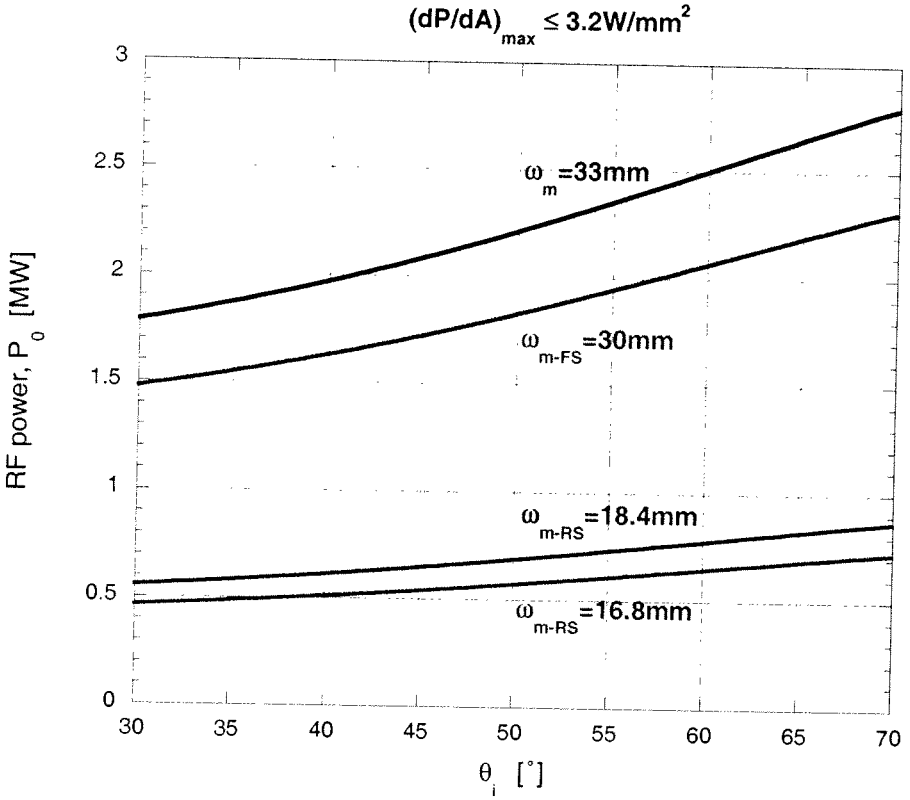

Given the above absorbed power fraction and peak power density limitation, a spot size of 33mm or large is needed on the plasma facing mirror for 2.0MW injection. Note, using the hypervapotron technique (increasing the allowable peak power density to $5W/mm^2$) would increase the injected power capabilities by 50% or between 0.9 and 1.1MW for the RS launcher.